

# Robust outlier detection for heterogeneous distributions applicable to censoring in functional MRI

Saranjeet Singh Saluja, Fatma Parlak and Amanda Mejia

## 1 Introduction

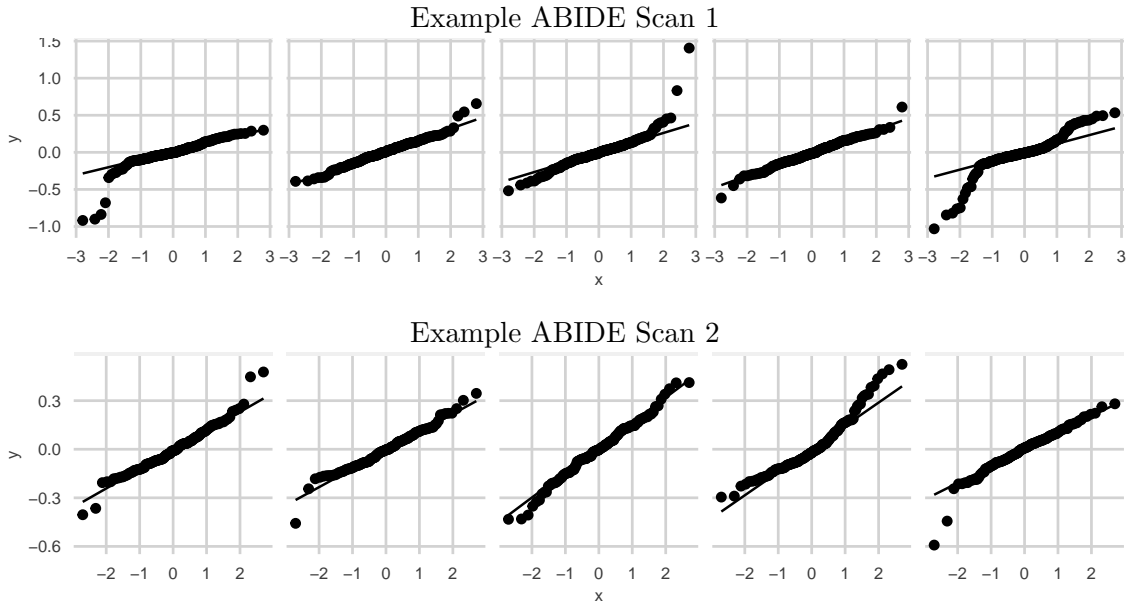
In neuroimaging data, small head movements, deep breaths and other physiological signals can induce artifacts into the data. Volumes in a functional magnetic resonance imaging (fMRI) time series thought to contain artifacts are often removed prior to statistical analysis to avoid the undue influence of artifactual signals on summary measures of brain function and connectivity. These volumes can be considered to be multidimensional statistical outliers, given their deviation from normal spatial patterns. While it is common practice to use measures of head motion and ad-hoc data driven measures to flag suspicious volumes (Power et al., 2014), a formal statistical outlier detection framework is desirable to optimize sensitivity and specificity.

Previous work has considered detection of contaminated fMRI volumes from a statistical outlier detection perspective. Afyouni and Nichols (2018) developed a statistically principled version of an existing measure, DVARS (the root mean square of subsequent volumes), providing a null distribution that can be used to detect abnormally high values with a certain degree of false positive control. Mejia et al. (2017) proposed a novel measure of abnormality based on dimension reduction, which was later improved upon by Pham et al. (2021) through the use of independent component analysis (ICA) and a robust version of kurtosis to extract components sensitive to outliers. Mejia et al. (2017) explored the use of robust multivariate outlier detection techniques for detecting statistically unusual values. Specifically, they considered the use of minimum covariance determinant (MCD) distances, a robust version of Mahalanobis distance, which have a known null distribution for Gaussian data (Hardin and Rocke, 2005). However, more recently Parlak et al. (2023) showed that the Gaussian assumption is not reasonable in this context and developed a

procedure that does not depend on Gaussianity. To demonstrate this, we employ the publicly accessible Autism Brain Imaging Data Exchange (ABIDE) initiative (Di Martino et al., 2014). This example dataset, included in the `fMRIScrub` R package, consists of a single brain slice from one session and is structured as a  $T \times V$  matrix, with  $T = 145$  time points and  $V = 4679$  voxels. Visual inspection of the raw fMRI scans indicates that the first session, derived from *ABIDE 1*, contains a considerable amount of artifact-related contamination, whereas the second session from *ABIDE 2* appears to exhibit minimal artifact presence. To evaluate the Normality assumption, Q-Q plots are provided for five randomly selected representative components in Figure 1. These plots clearly show that extracted components exhibit a variety of non-Gaussian distributional shapes, including skewness and heavy tails.

The multivariate technique of Parlak et al. (2023) relies on a univariate outlier detection and imputation step within each extracted component. Specifically, they compute a robust z-score using the median and median absolute deviation (scaled to be unbiased for the standard deviation) and flag any observations with magnitude exceeding a certain value. This can be considered a robust version of the “empirical rule” for near-Normally distributed data. However, this procedure may have poor performance at identifying univariate outliers for non-Gaussian components. There is a need for a robust technique applicable to a variety of distributional shapes. This current study addresses this gap by developing a novel, robust transformation to Normality, after which the empirical rule can be safely applied.

Data transformation approaches are commonly utilized to satisfy an assumption of Normality. One well-known family of transformation is the Box-Cox power transformations (Tukey, 1957; Box and Cox, 1964). Since this power transformation requires the data to be positive, Yeo and Johnson (2000) proposed a modified transformation applicable to data on the real line. The transformation parameter in these methods is typically obtained using the maximum likelihood estimate, which is known to be sensitive to outliers. The influence of outliers on such transformations can therefore lead to masking, where a true outlier appears to be a regular observation, or swamping, where a regular observation appears to be an outlier. Recently, Raymaekers and Rousseeuw (2021) developed a robust version of the Box-Cox and Yeo-Johnson transformations. However, this approach is only applicable to certain types of skewed distributions and may fail for other distributional shapes, such as heavy-tailed or light-tailed symmetric distributions.



(a) Normal QQ-plots of several components for ABIDE1 (out of 26) and ABIDE2 (out of 5)

Figure 1: **Functional MRI extracted components violate the Gaussianity assumption.** Normal QQ plots of five randomly selected components extracted using the ICA-based method of Pham et al. (2021) from two example fMRI scans from the ABIDE dataset. These show a variety of non-Gaussian distributional shapes, as well as the presence of outliers.

Here, we develop a robust transformation to standard Normality applicable to a wide variety of distributional shapes, based on the sinh-arcsinh (SHASH) family of distributions. After applying this transformation, identification of outliers becomes straightforward via quantiles of the standard Normal distribution. The remainder of the paper proceeds as follows. First, the robust transformation procedure is introduced and explained in detail. Next, the efficacy of the proposed method is assessed through simulation studies conducted under various scenarios. Finally, the simulation results are summarized, and a discussion is provided addressing potential limitations and outlining directions for future research.

## 2 Methods

The proposed method is based on the sinh-arcsinh (SHASH) family of distributions introduced by Jones and Pewsey (2009). This versatile distribution family is characterized by four parameters controlling the mean ( $\mu$ ), variance ( $\sigma$ ), skewness ( $\nu$ ), and tailweight ( $\tau$ ). The most basic form of the SHASH distribution family is obtained by applying an inverse SHASH transformation to a standard

Normal random variable. Letting  $Z$  be standard Normal random variable,  $X_{\nu,\tau} = S_{\nu,\tau}^{-1}(Z)$  is said to follow a SHASH distribution with skewness  $\nu$  and tailweight  $\tau$ . The SHASH transformation  $S_{\nu,\tau}$  and its inverse  $S_{\nu,\tau}^{-1}$  are defined as:

$$S_{\nu,\tau}(X_{\nu,\tau}) = \sinh(\tau \sinh^{-1}(X_{\nu,\tau}) - \nu) \quad (1)$$

$$S_{\nu,\tau}^{-1}(Z) = \sinh(\tau^{-1}(\sinh^{-1}(Z) + \nu)) \quad (2)$$

Therefore a density function of a SHASH distribution is

$$f_{\nu,\tau}(x) = \frac{\tau(1 + (S_{\nu,\tau}^2(x))^{1/2})}{(2\pi(1 + x^2))^{1/2}} \exp\left(\frac{-S_{\nu,\tau}^2(x)}{2}\right) \quad (3)$$

Since a standard normal random variable is a standardization of a random variable by subtracting its mean and dividing by its standard deviation, the parameters  $\mu$  and  $\sigma$  can be incorporated into the equation resulting in a 4 parameter family. Under the regularity conditions of maximum likelihood theory, Jones and Pewsey (2009) demonstrated that in this 4-parameter SHASH family, the estimation of the mean is asymptotically independent of the scale and tailweight parameters, but the scale and tailweight parameters are asymptotically dependent. Jones and Pewsey (2009) alleviate this asymptotic correlation by a reparametrization, replacing  $\sigma$  with  $\sigma\tau$  in the density. This gives rise to what is referred to as the SHASHo2 distribution Rigby et al. (2019), which is implemented in the `gamlss.dist` R package. In this study, the SHASHo2 (hereafter referred to as “SHASH”) family of distributions is employed, whose probability density function is:

$$f_X(x|\mu, \sigma, \nu, \tau) = \frac{c(x)\tau}{\sqrt{2\pi}\sigma(1 + w^2(x))^{1/2}} \exp(-r^2(x)/2) \quad (4)$$

where  $w = (x - \mu)/(\sigma\tau)$  and

$$r = \frac{1}{2}\{\exp[\tau \sinh^{-1}(w)] - \exp[-\nu \sinh^{-1}(w)]\} \quad (5)$$

$$c = \frac{1}{2}\{\tau \exp[\tau \sinh^{-1}(w)] + \nu \exp[-\nu \sinh^{-1}(w)]\}. \quad (6)$$

Note that  $r$  and  $c$  are simplified and equivalent expressions derived from the original SHASH transformation (1). The ranges and interpretations of each of the four parameters  $(\mu, \sigma, \nu, \tau)$  are summarized in **Table 1**.

Parameter	Range	Function
$\mu$	$-\infty < \mu < \infty$ ,	modulates the mean
$\sigma$	$0 < \sigma < \infty$ ,	modulates the variance
$\nu$	$-\infty < \nu < \infty$ ,	modulates the skewness
$\tau$	$0 < \tau < \infty$ ,	modulates the tailweight

Table 1: Range and function of each parameter in the SHASH( $\mu, \sigma, \nu, \tau$ ) distribution.

To illustrate the influence of the four parameters  $(\mu, \sigma, \nu, \tau)$  on the shape of a SHASH distribution, **Figure 2** shows five different 4-parameter SHASH distributions, based on a random sample of  $n = 1000$  from each distribution. In the top panel, densities and Normal QQ plots for the five distributions are shown, along with the four parameter values. Comparing the heavy-tailed to the light-tailed distribution,  $\tau$  is the only parameter that changes: the value increases from 0.5 to 10, illustrating that higher values ( $\tau > 1$ ) produce light tails while lower values ( $\tau < 1$ ) produce heavy tails. Similarly, comparing the left-skewed and right-skewed distributions,  $\nu$  is the only parameter that changes, from  $-2$  to  $2$ . Negative values of  $\nu$  produce a left-skewed distribution, while positive values of  $\nu$  produce a right-skewed distribution. With the same magnitude of  $\nu$ , the skewness strength is equal.

Recall that SHASH random variables are transformed to standard Normal random variables by applying the SHASH transformation given in Equation 1. The bottom panel of **Figure 2** displays the distributions and Normal QQ plots after applying the SHASH transformation with the corresponding parameters. As expected, the data after transformation clearly follow a standard Normal distribution.

Given the flexibility of the SHASH distribution family to represent widely heterogeneous distributional shapes, including heavy or light tails and/or skew, our approach is based on the assumption that the underlying data can be modeled using a SHASH distribution. **Figure 3** illustrates the use of the SHASH transformation on several different well-known distributions. Most of these do not fall within the SHASH family. However, applying the SHASH transformation using estimated SHASH parameters brings all the distributions much closer to Normality. In the case of the Normal

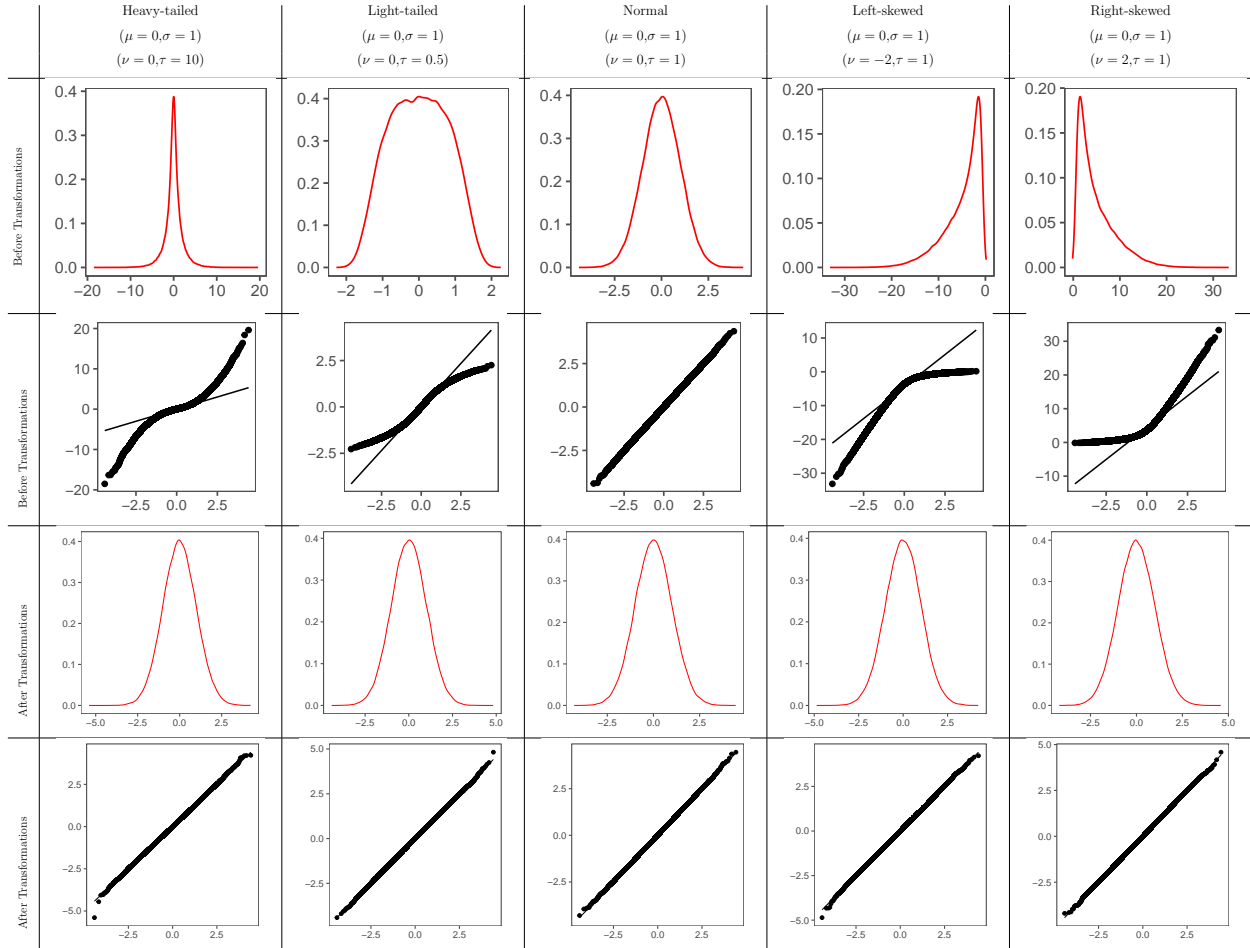


Figure 2: **Example SHASH random variables and their transformation to Normality.** Each data set contains 100000 randomly sampled draws from a SHASH distributions with given parameter values. These represent a variety of distributional shapes: heavy-tailed, light-tailed, Normal, left-skewed, and right-skewed, respectively. For each random variable, an estimated density curve and Normal Q-Q plot before and after transformation to Normality is shown. The bottom panel illustrates how SHASH random variables can be transformed to standard Normal random variables through the SHASH transformation.

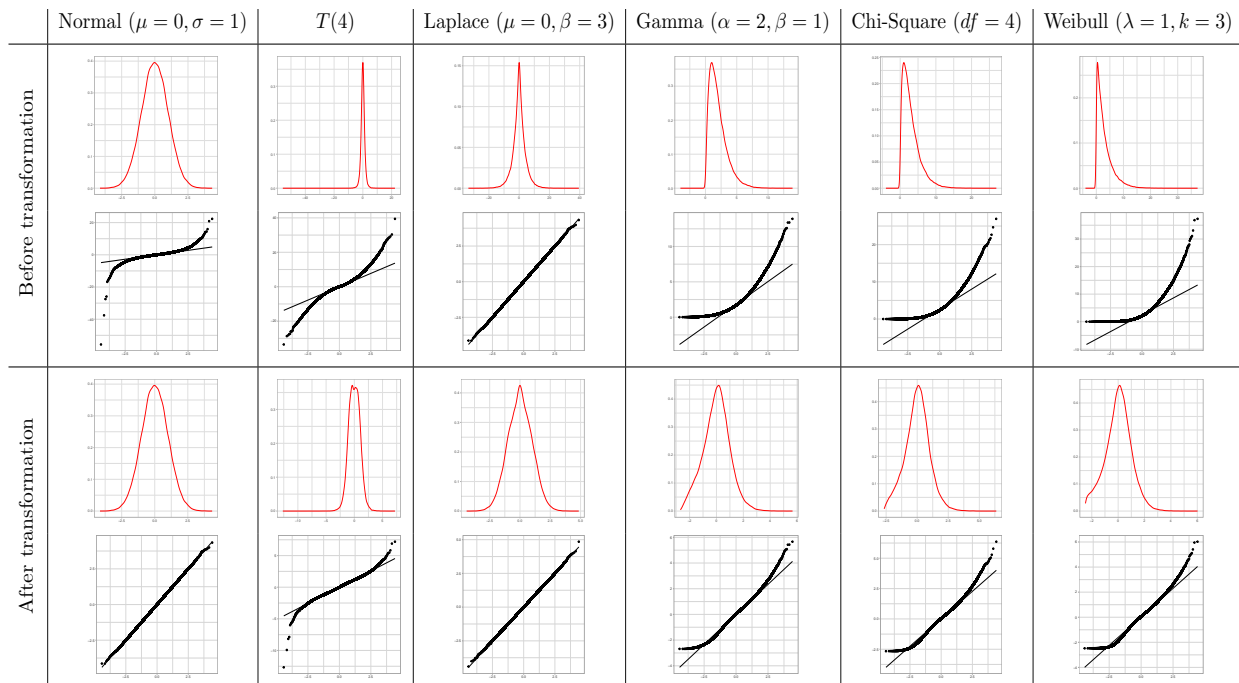


Figure 3: **Illustration of applying SHASH transformation to non-SHASH distributions.** Each distribution was modeled as a SHASH random variable, although most distributions shown here do not fall within the SHASH family of distributions. The bottom panel shows the distributions after applying SHASH transformation using maximum likelihood estimates of the SHASH parameters. While only the Normal and  $t$  distributions are perfectly transformed, the other example distributions (Laplace, Gamma, Chi-squared and Weibull) become much closer to Normal than before transformation.

and  $t$  distributions, the random variables are perfectly Normally distributed after applying SHASH transformation.

Our proposed robust SHASH-based transformation and outlier detection procedure involves the following steps, following a similar approach to Raymaekers and Rousseeuw (2021) for Box-Cox and Yeo-Johnson transformations. These steps are implemented in the open source `fMRIscrub` R package, version 0.13.0.

1. Initialize outlier labels using existing robust techniques, described below.
2. Model the data using a SHASH distribution, using maximum likelihood estimation (MLE) to obtain SHASH parameter estimates (Jones and Pewsey, 2009), excluding labeled outliers to avoid their undue influence.
3. Apply SHASH-to-Normal transformation (Equation 1) using the estimated parameters.
4. Identify observations as outliers if their transformed values exceed a specified threshold un-

likely to occur under standard Normal distribution. Here we adopt a threshold of  $\pm 3$  (or  $+3$  if the original data is strictly positive).

5. Iterate steps 2-4, excluding previously identified outliers from parameter estimation, until convergence, defined as no change in the identified set of outlier observations.

At step 1, outliers are initialized using existing robust procedures. This is a crucial step, given the high degree of flexibility of the SHASH distribution. If outliers are allowed to influence the SHASH parameter estimates, they are likely to have a strong effect, leading to masking of true outliers after normalization. Several existing robust techniques are available in `fMRIscrub`: robust z-scoring, robust asymmetric z-scoring, and Huber z-scoring. For each of these, a z-score is computed by subtracting a robust estimate of location and dividing by a robust estimate of scale. Following Raymaekers and Rousseeuw (2021), observations exceeding the 0.995 quantile of the standard Normal distribution, equal to 2.58, are initialized as outliers. For robust z-scoring and robust asymmetric z-scoring, the median,  $m_x$ , is used as the estimate of location, and a version of median absolute deviation (MAD) is used as the estimate of scale. Define  $MAD_x = 1.4826 \text{ med}(|x_i - m_x|)$ , which is consistent for the standard deviation under Normality (Ruppert, 2010, p. 118). In the case of asymmetric z-scoring, we compute the MAD for the left and right tails separately, i.e.  $MAD_{x,l} = 1.4826 \text{ med}(|x_i - m_x| : x_i \leq m_x)$  for the left tail, and likewise for the right tail. For Huber z-scoring, Huber M-estimators of the location and scale are used (Huber, 1981), as in Raymaekers and Rousseeuw (2021). In this work, we adopt symmetric robust z-scoring for initial outlier detection.

### 3 Simulation

To evaluate the performance of our proposed SHASH-based outlier detection procedure in a variety of scenarios, we perform an extensive simulation study, where the true outliers are known. For comparison, we also apply two existing methods: robust z-scoring (“empirical rule”) and robust Yeo-Johnson transformation (Raymaekers and Rousseeuw (2021) (“YJ”). For all methods, we use a final outlier detection threshold of  $\pm 3$  (or  $+3$  for positively valued data).

We consider data arising from several parametric distributions, and we vary the degree of out-

lier contamination with outliers from light (1%) to heavy (30%). We consider two main categories of distributions: (1) symmetric distributions with support on  $(-\infty, \infty)$  and (2) right-skewed distributions with support on  $(0, \infty)$ . Table 2 lists the distributions, their parameter values, and the rationale for their inclusion in the study. Since the robust empirical rule is designed for Normally distributed data, it is expected have better performance in symmetric versus asymmetric distributions and optimal performance for Gaussian data. Since robust YJ transformation is designed to deal with skew, it is expected to have better performance in asymmetric versus symmetric distributions.

Distribution Type	Distribution	Parameters	Purpose
Real-line	Normal( $\mu, \sigma$ )	$\mu = 0, \sigma = 1$	Optimal case for empirical rule
	Student's $t(\nu)$	$\nu = 4$	Heavy-tailed
	Laplace( $\mu, \beta$ )	$\mu = 0, \beta = 3$	Exponential shape
Positive-valued	Gamma( $\alpha, \beta$ )	$\alpha = 2, \beta = 1$	Right-skewed, positive-only distribution
	Chi-square( $\chi$ )	$\chi = 3$	Right-skewed with moderately heavy tails
	Weibull( $\lambda, k$ )	$\lambda = 1, k = 3$	Skewed with lighter tails

Table 2: Summary of distributions used in the simulation study, along with selected parameters and evaluation purpose.

For each scenario considered, we perform 100 independent simulation repetitions, each with a fixed sample size of  $n = 500$ . We induce outliers by first transforming the distribution to be approximately Normal, then replacing a randomly selected fraction of each dataset with larger-magnitude values. Those values are sampled from a scaled and shifted chi-square distribution, as described next. For distributions defined on the real line, outliers are randomly assigned positive or negative signs.

### 3.1 Outlier Generation

Figures 4 and 5 illustrate the process of generating outlier-contaminated data for each type of distribution. The first column shows a randomly sample of 500 with no outliers. Using a large sample from the same distribution, the data is modeled as a SHASH distribution to obtain MLEs of the SHASH parameters. The second column shows the data after applying the SHASH transformation to approximately achieve standard Normality. The third column shows the transformed data after randomly replacing 10% of the observations with outliers. These outliers are generated by sampling

from a Chi-square distribution with 4 degrees of freedom, scaling by a factor of  $\frac{1}{6}$ , and subsequently shifting by 4 units, i.e.,  $\frac{\chi^2(4)}{6} + 4$ . Finally, as shown in the fourth column, the data contaminated with outliers is reverse-transformed back to the original distribution.

### 3.2 Evaluation Metrics

For each method of outlier detection, accuracy is evaluated by comparing the flagged outliers against the true outliers in each simulated dataset. Two performance metrics are used: the True Positive Rate (TPR) or sensitivity, and the False Positive Rate (FPR).

True positives (TP) are truly outlying observations that are correctly identified as outliers, while false positives (FP) are truly non-outlying observations that have been incorrectly flagged as outliers. Likewise, true negatives (TN) are truly non-outlying observations correctly classified as non-outliers, while false negatives (FN) are true outliers not identified as outliers. The true positive rate  $TPR = TP/(TP + FN)$  quantifies the method’s ability to correctly identify actual outliers. A higher TPR indicates the ability of the method to identify actual outliers. A TPR close to 1.0 is desirable, indicating that the method detects most of the true outliers. The false positive rate  $FPR = FP/(FP + TN)$  quantifies the proportion of truly non-outlying observations incorrectly identified as outliers by the method. A low FPR is desirable as it indicates minimal misclassification of non-outlying data observations as outliers. If the data is perfectly transformed to Normality, the false positive rate (FPR) should be approximately equal to 0.003, since this is the proportion of standard Normal data observations falling beyond  $\pm 3$ .

## 4 Results

In this section, we visually and quantitatively evaluate the performance of our proposed SHASH-based robust outlier detection technique, compared with the robust empirical rule and robust YJ transformation. We first show several randomly selected examples of each method using histograms and QQ-plots to provide visual intuition for each method. We then summarize the performance of each method in terms of FPR and TPR or sensitivity.

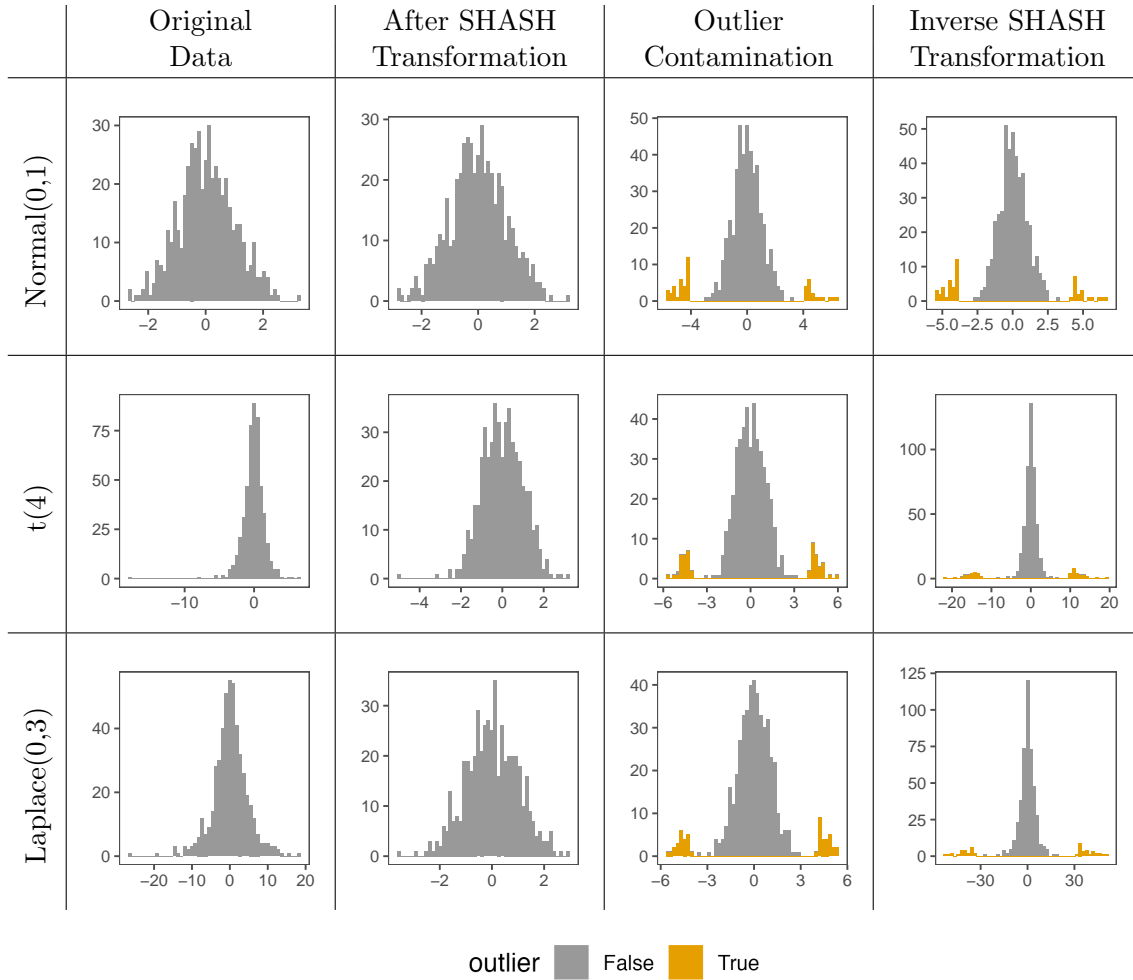


Figure 4: **Illustration of outlier contamination process for real-line distributions.** The first column shows the outlier-free sample. The second column shows the outlier-free data after applying a SHASH transformation to approximately achieve standard Normality. In the third column, outliers originating from a different distribution are induced by replacing 10% of the data with values randomly sampled as  $\chi^2(4)/6 + 4$ , as illustrated in the third column. The sign of each outlier is randomly assigned. Finally, in the fourth column, the outlier contaminated data is reverse-transformed to the original scale and distribution.

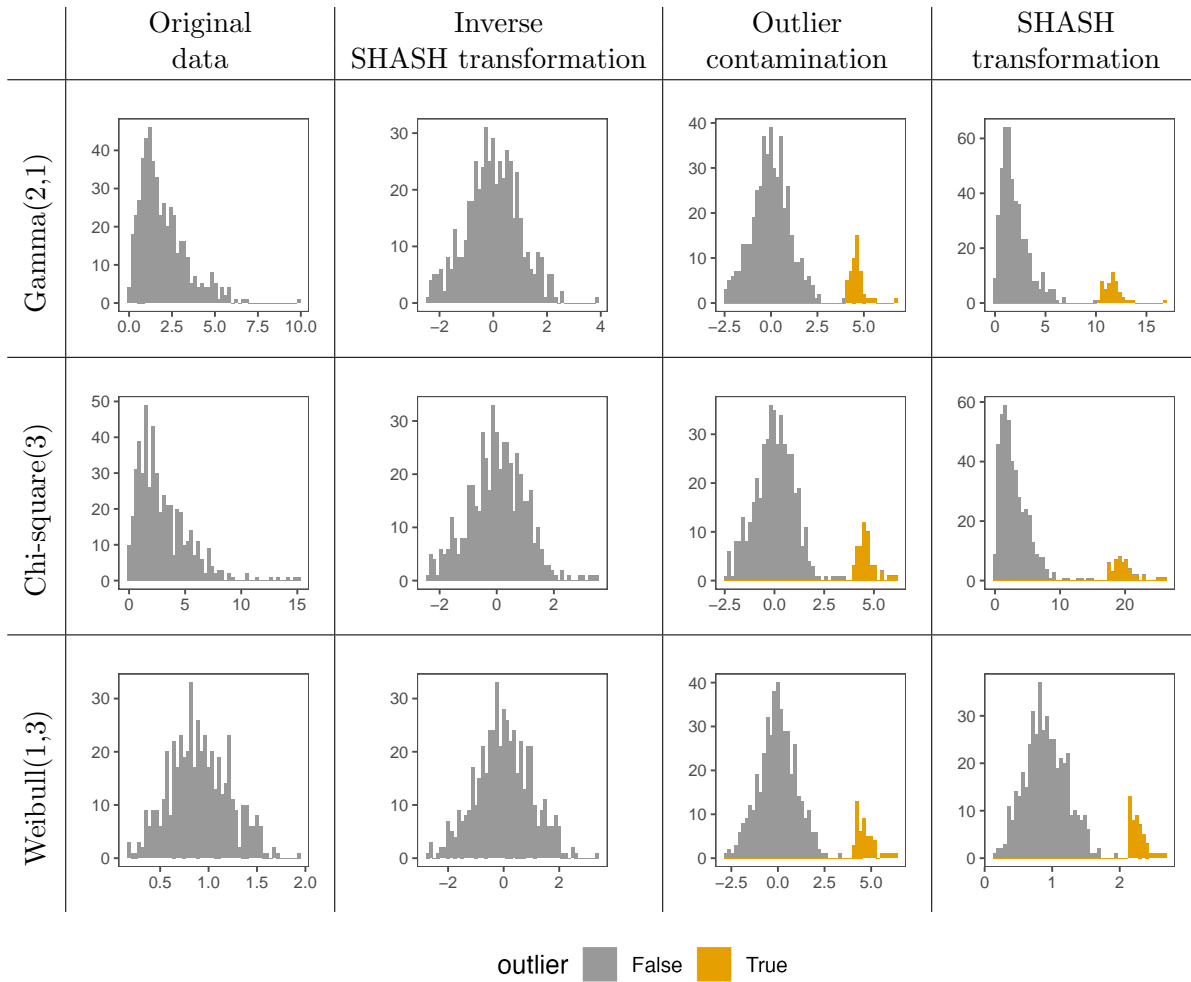


Figure 5: **Illustration of outlier contamination process for positively-valued distributions.** The first column shows the outlier-free sample. The second column shows the outlier-free data after applying a SHASH transformation to approximately achieve standard Normality. In the third column, outliers originating from a different distribution are induced by replacing 10% of the data with values randomly sampled as  $\chi^2(4)/6 + 4$ , as illustrated in the third column. Finally, in the fourth column, the outlier contaminated data is reverse-transformed to the original scale and distribution.

## 4.1 Example Visualizations

**Figures 6** and **7** show one randomly selected example dataset for each of the six distributions considered in the simulation study. Outlying observations are shown in red. The first column shows the data after robustly z-scoring; the second column shows the data after applying robust YJ transformation; and the third column shows the data after applying our robust SHASH transformation. Vertical lines indicate the outlier detection threshold(s). After a successful transformation, the data should will approximately follow a standard Normal distribution, and outliers will fall outside the thresholds while non-outliers will fall within them.

**Figure 6** shows that all three methods perform well when the data follow a Normal distribution, as expected. There is a clear distinction between outliers and regular observations. Note that if the data is known to follow a Normal distribution, then no transformation is needed. However, in many cases we may not have this knowledge a-priori, so by applying transformation to Normally-distributed data, we are evaluating whether there is a detrimental effect of transformation.

Turning to the  $t$  distribution, due to its heavy tails both the empirical rule and YJ misclassify some non-outliers as outliers. The YJ transformation is not equipped to transform the  $t$  distribution to Normality, since it is designed to eliminate skew. Similarly, in the Laplace distribution the empirical rule and YJ methods tend to mislabel non-outliers in the tails as outliers. For both the  $t$  and Laplace distributions, in these examples SHASH transformation appears to do a good job of transformation to Normality and largely avoids misclassification of regular observations as outliers.

For skewed distributions, shown in **Figure 7**, the empirical rule not surprisingly seems to perform poorly, misclassifying several regular observations in the tail as outliers. More surprisingly, YJ transformation fails in these examples for all three distributions. The true outliers fall well below the outlier detection threshold, a result of masking of outliers due to their influence on the transformation. Since the robust YJ transformation relies on Huber estimators of location and scale to identify outliers during the transformation, it may be that under these simulation conditions those estimators are not sufficiently robust. By contrast, SHASH transformation achieves a nearly symmetric distribution, with outliers far into the upper tail. While some regular observations are still misclassified as outliers, they are fewer than prior to transformation.

To more clearly show the Normality or non-Normality of the data distributions, **Figures 8** and

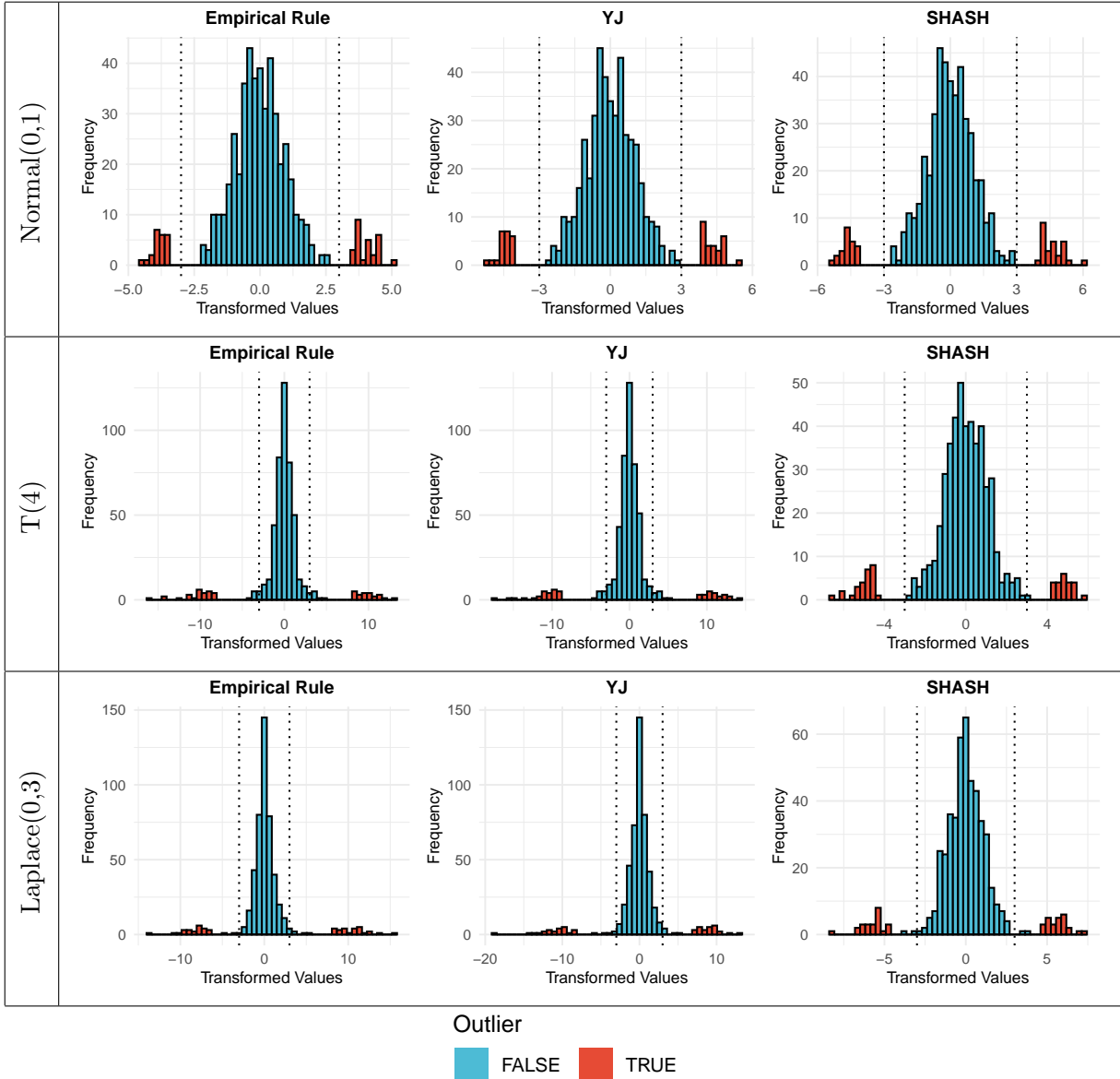


Figure 6: Example histograms of transformed values by robust empirical rule, YJ transformation, and SHASH transformation for real-line distributions. For each distribution, one randomly selected example dataset is shown. Vertical lines indicate the outlier detection thresholds, and true outliers are shown in red.

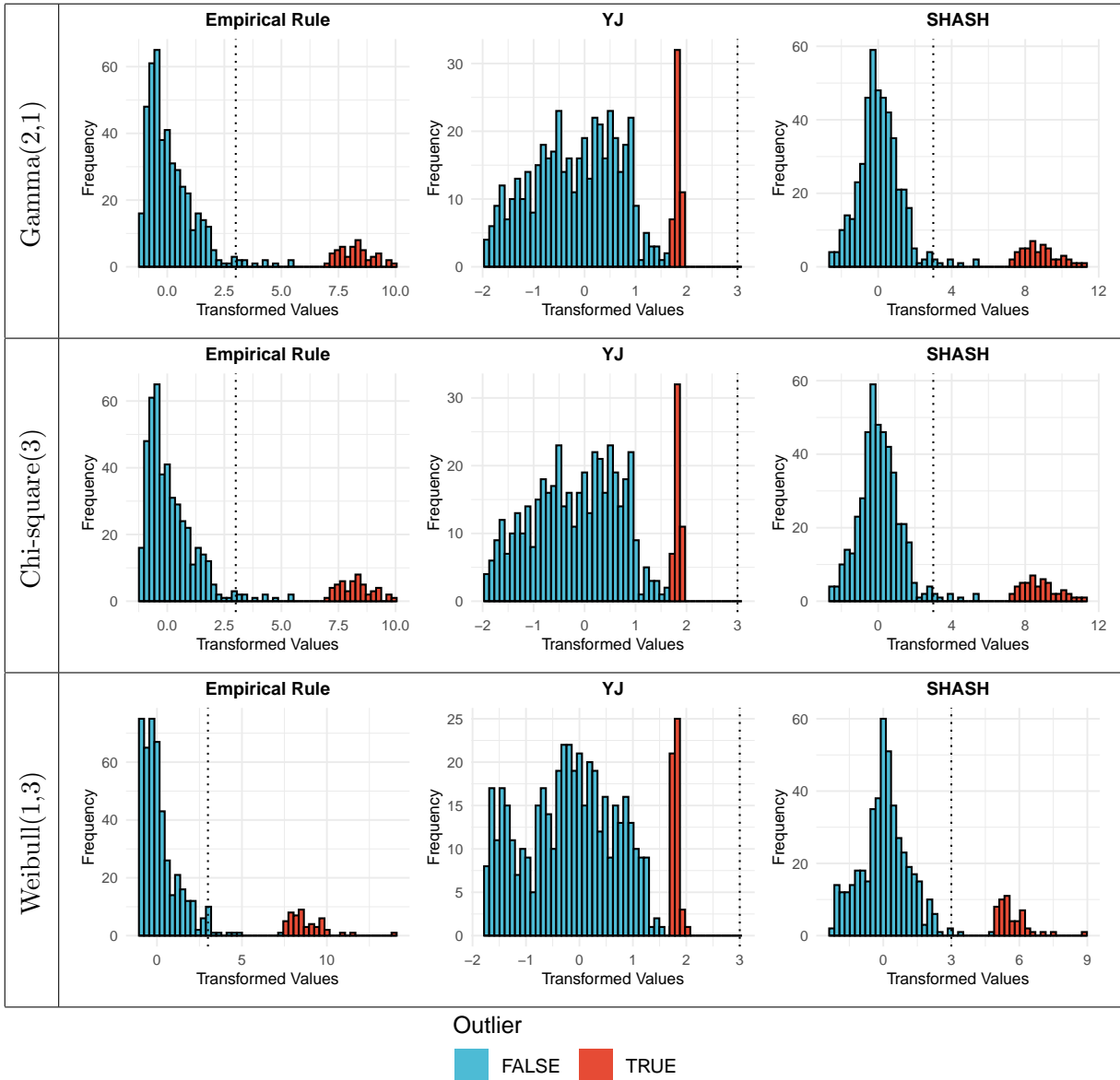


Figure 7: Example histograms of transformed values by robust empirical rule, YJ transformation, and SHASH transformation for positively-valued distributions. For each distribution, one randomly selected example dataset is shown. Vertical lines indicate the outlier detection thresholds, and true outliers are shown in red.

**9** show Normal QQ plots for each distribution and method. For each distribution, three randomly selected example simulated datasets are shown. The first column corresponds to the same datasets shown in Figures 6 and 7. Here, true outliers are excluded to show the efficacy of transformation to Normality for the true distribution.

Examining **Figure 8**, for the Normal distribution, both YJ and SHASH transformation sometimes distort the distribution slightly, bringing some regular observations beyond the outlier detection threshold. For the t and Laplace distributions, however, SHASH transformation tends to do a good job of achieving approximate Normality and avoiding misclassification of regular observations as outliers. The heavier tails in these distributions are problematic for both the empirical rule and YJ transformation, with a sizeable number of regular observations falling beyond the outlier detection thresholds.

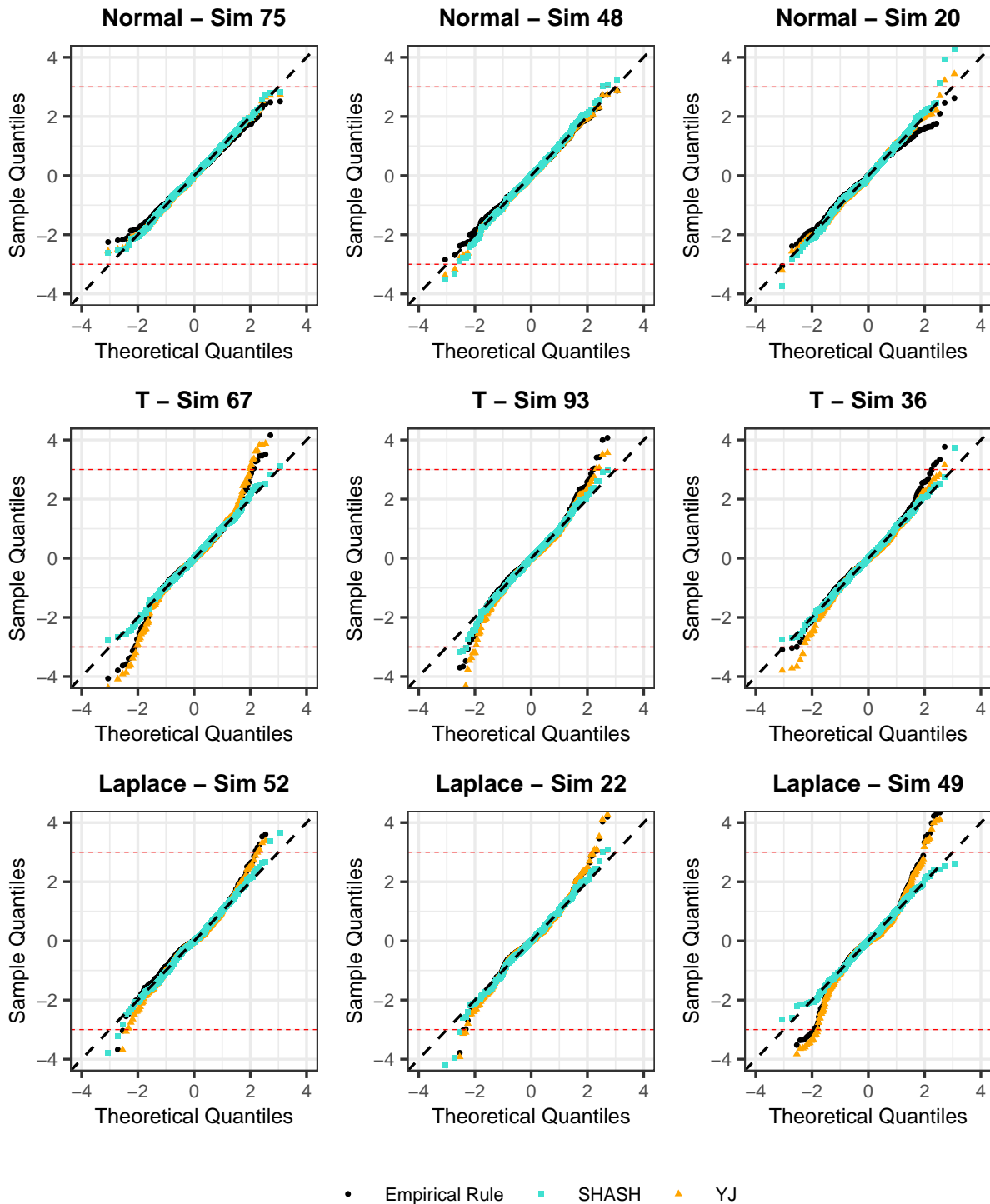


Figure 8: **Normal QQ plots for symmetric real-line distributions.** Only non-outlying observations are displayed in order to clearly show whether Normality has been successful. For each distribution, three simulated datasets were randomly selected, each with 10% contamination of outliers. The first column corresponds to the same datasets shown in the histograms above.

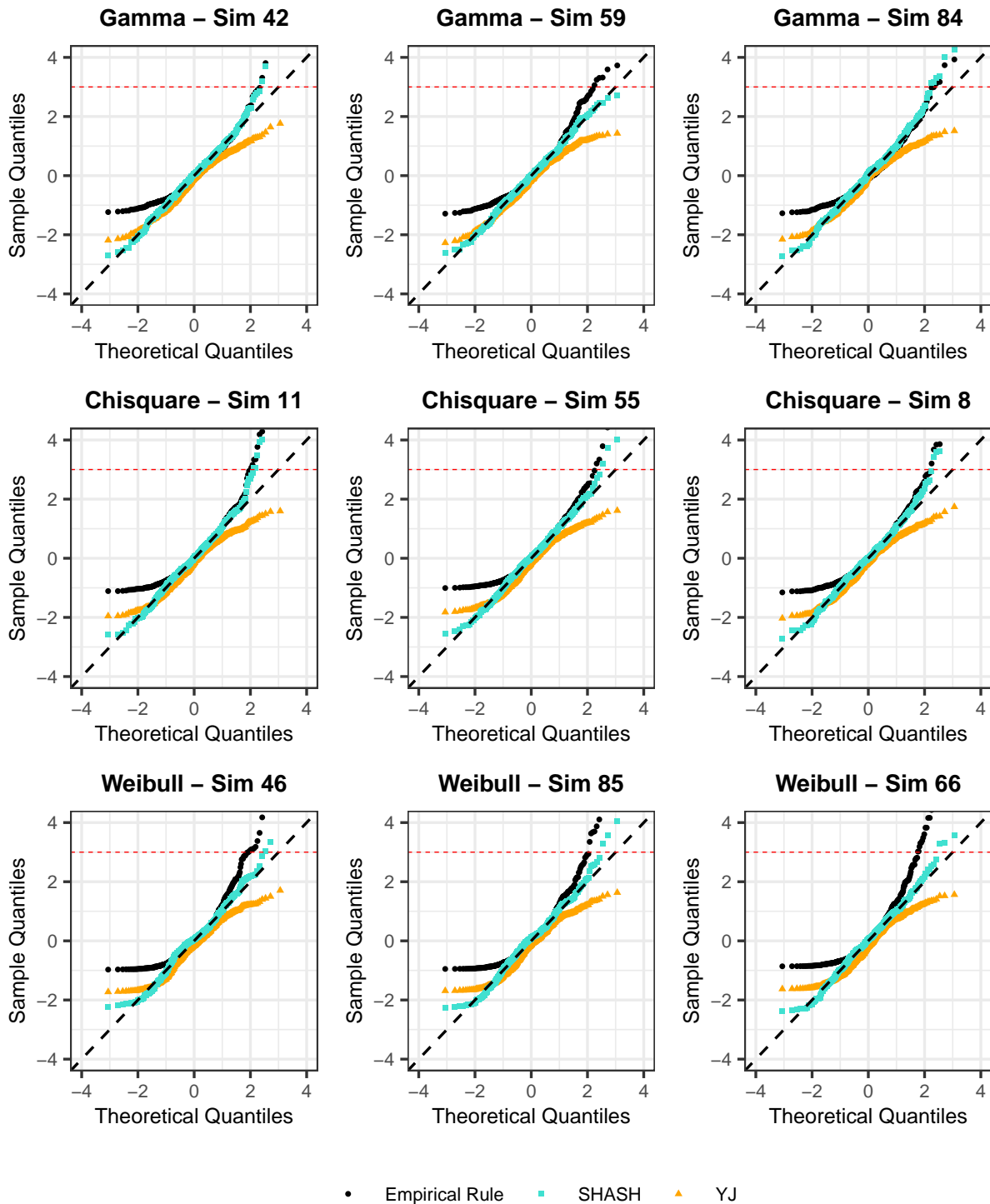


Figure 9: Normal QQ plots for positively-valued, right-skewed distributions. Only non-outlying observations are displayed in order to clearly show whether Normality has been successful. For each distribution, three simulated datasets were randomly selected, each with 10% contamination of outliers. The first column corresponds to the same datasets shown in the histograms above.

Turning to **Figure 9**, for skewed distributions we observe more variation in performance across methods. SHASH tends to corrects the skew fairly well in most cases. In contrast, YJ often over-corrects the skew, resulting in a short-tailed distribution after transformation. As discussed above, this may be due to the undue influence of outliers on the YJ transformation due to the use of Huber estimators of location and scale. Unsurprisingly, the empirical rule does not remove the skew in these distributions, generally resulting in high rates of misclassification of regular observations as outliers.

## 4.2 Quantitative Performance Evaluation

**Figure 10** shows the TPR and FPR of each outlier detection method, averaged over 100 simulated datasets, for each distribution and outlier contamination level. Our SHASH-based outlier detection procedure demonstrates generally strong performance across a range of distributions. With very heavy outlier contamination (30%), the performance of SHASH suffers, likely due to the influence of outliers on the transformation procedure. However, up to an contamination level of 20%, SHASH generally achieves lower false positive rates compared with the empirical rule while maintaining high sensitivity to outliers.

Focusing first on the symmetric real-line distributions, SHASH achieves the best performance with the exception of Normally distributed data or very heavy contamination. For the Normal distribution, all three methods achieve near-perfect sensitivity (TPR near 1) when outlier contamination is  $\leq 10\%$ , but SHASH transformation leads to inflated FPR for lower contamination levels. At 20% contamination, SHASH actually outperforms the empirical rule and YJ transformation, maintaining high sensitivity and a low false positive rate. Turning to the heavy-tailed real-line distributions (t and Laplace), all three methods achieve near-perfect sensitivity when the outlier contamination is  $\leq 20\%$ , but the false positive rate is above the nominal level. SHASH outperforms the other methods by maintaining near-perfect sensitivity while lowering the false positive rate.

Turning to the skewed, positively-valued distributions, SHASH and the empirical rule achieve near-perfect sensitivity up to 20% contamination. Again the performance of SHASH suffers under very high contamination, likely due to the influence of outliers on the transformation. The YJ method performs poorly in most cases, with sensitivity near zero. Considering the FPR, SHASH generally outperforms the empirical rule at controlling false positives up to 20% contamination.

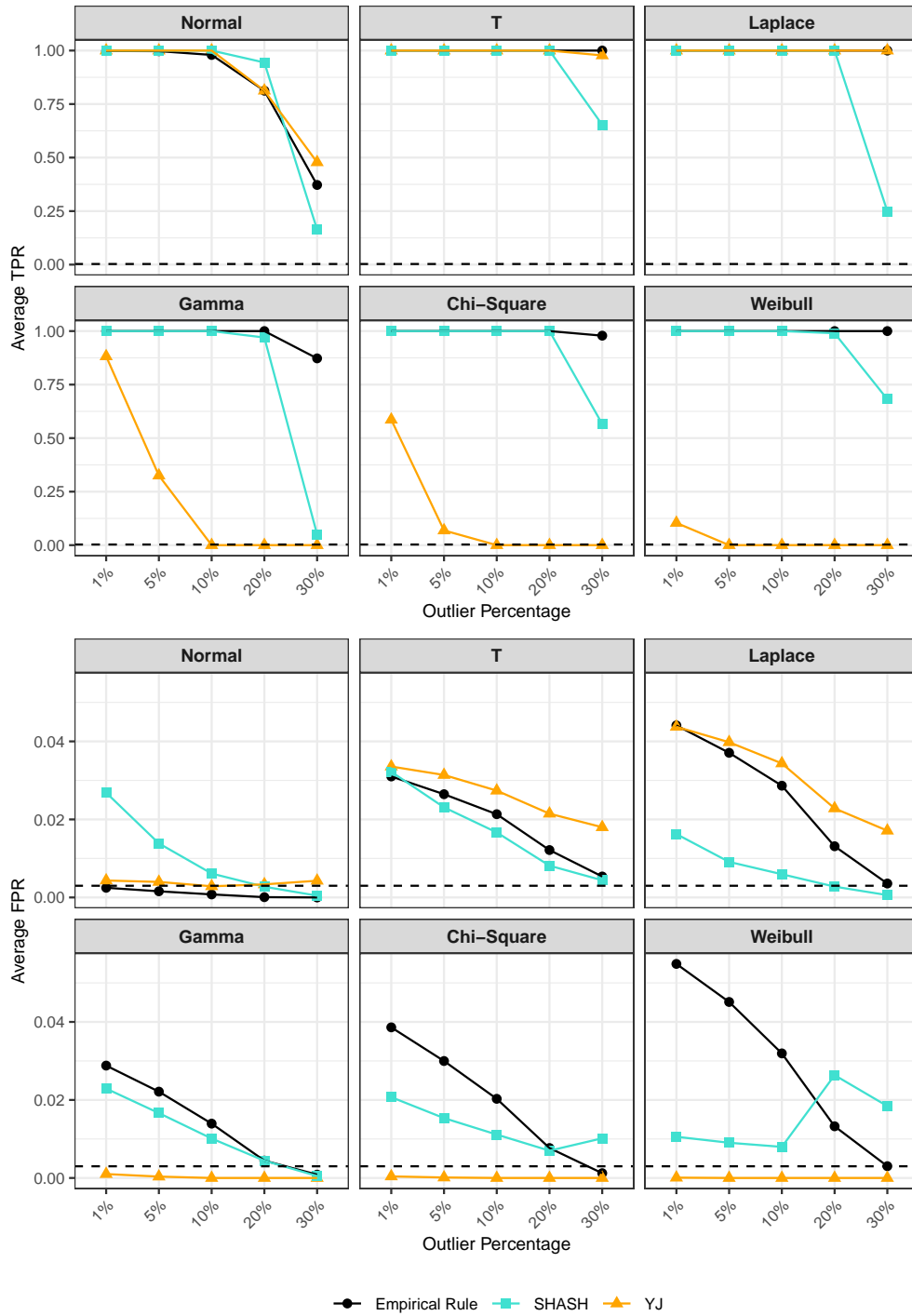


Figure 10: **Accuracy of outlier detection in simulation study.** True positive rate (TPR), i.e. sensitivity, and false positive rate (FPR) (mean over 100 simulations) across distributions and outlier contamination levels for three robust outlier detection methods: empirical rule, YJ transformation, and SHASH transformation. The horizontal line indicates the nominal false positive rate of 0.003.

## 5 Discussion

In this work, we have developed a novel robust outlier detection method based on the flexible sinh-arcsinh (SHASH) family of distributions. Using simulated data from a range of non-Gaussian and Gaussian distributions, we benchmarked its performance against two existing methods: robust z-scoring or the “empirical rule”, and a robust Yeo-Johnson transformation-based approach recently proposed by (Raymaekers and Rousseeuw, 2021). Using simulated datasets contaminated with outliers at varying proportions, robust SHASH transformation demonstrated consistently strong performance across most scenarios, with the notable exception of very heavy outlier contamination.

For low to moderate outlier contamination levels, the proposed SHASH outlier detection method consistently achieved high sensitivity while maintaining low false positive rates (FPRs close to or below the theoretical threshold of 0.003). These improvements were most notable in skewed or heavy-tailed distributions. In contrast, the empirical rule frequently misclassified regular observations as outliers, leading to inflated FPRs, particularly in non-Normal settings. The YJ method exhibited poor sensitivity in skewed distributions.

SHASH’s performance declines under heavy contamination (20–30%), particularly in positive distributions. This is likely due to the influence of outliers on the transformation, which is sensitive to outliers given the high degree of flexibility in the SHASH parameterization. This reflects a dependency of the proposed techniques on initial outlier flags, which is an important limitation. The robust empirical rule employed for initial weighting is inherently limited, due to its assumption of approximate symmetry and normality. Consequently, distributions exhibiting substantial skewness, such as Gamma or Weibull, can lead to ineffective initial weight assignments. Thus, improving the efficacy of this novel SHASH-based approach is highly dependent on enhancing the initial outlier identification step.

To address this shortcoming, a promising alternative could be to adopt the Isolation Forest algorithm (Liu et al., 2008) for generating initial outlier weights. Isolation Forests are based on the principle that outliers are easier to isolate in random partitions of the data compared to normal observations. This property is particularly advantageous because it does not require explicit assumptions about the distributions, symmetry, or underlying parameterizations of the data. By employing Isolation Forest for initial outlier flagging, observations likely to contaminate the param-

eter estimation step can be reliably identified without restrictive distributional assumptions. This flexibility is crucial for the SHASH-based methodology, which is particularly sensitive to contamination during initial transformation parameter estimation

Additionally, analyses were conducted exclusively on simulated datasets, potentially limiting the direct application and generalizability of findings. Future research should evaluate the proposed method on real-world data sets, particularly functional magnetic resonance (fMRI) data, which motivated the present research, to validate the practical effectiveness of the method. Application to real and toy data would enable assessment of the method's performance in more complex and varied environments.

Finally, extending this robust univariate approach to higher-dimensional, multivariate contexts would be a compelling future research direction. Given the multidimensional nature of neuroimaging data, a multivariate adaptation of the SHASH-based framework could enable more holistic and accurate artifact detection and correction, further improving the reliability and quality of subsequent neuroimaging analyses.

## References

- Afyouni, S. and Nichols, T. E. (2018). Insight and inference for dvars. *Neuroimage*, 172:291–312.
- Box, G. E. and Cox, D. R. (1964). An analysis of transformations. *Journal of the Royal Statistical Society: Series B (Methodological)*, 26(2):211–243.
- Di Martino, A., Yan, C.-G., Li, Q., Denio, E., Castellanos, F. X., Alaerts, K., Anderson, J. S., Assaf, M., Bookheimer, S. Y., Dapretto, M., et al. (2014). The autism brain imaging data exchange: towards a large-scale evaluation of the intrinsic brain architecture in autism. *Molecular psychiatry*, 19(6):659–667.
- Hardin, J. and Rocke, D. M. (2005). The distribution of robust distances. *Journal of Computational and Graphical Statistics*, 14(4):928–946.
- Huber, P. J. (1981). *Robust Statistics*. John Wiley & Sons.
- Jones, M. C. and Pewsey, A. (2009). Sinh-arcsinh distributions. *Biometrika*, 96(4):761–780.

- Liu, F. T., Ting, K. M., and Zhou, Z.-H. (2008). Isolation forest. In *2008 Eighth IEEE International Conference on Data Mining*, pages 413–422. IEEE.
- Mejia, A. F., Nebel, M. B., Eloyan, A., Caffo, B., and Lindquist, M. A. (2017). Pca leverage: outlier detection for high-dimensional functional magnetic resonance imaging data. *Biostatistics*, 18(3):521–536.
- Parlak, F., Pham, D. D., and Mejia, A. F. (2023). A robust multivariate, non-parametric outlier identification method for scrubbing in fMRI.
- Pham, D., McDonald, D., Ding, L., Nebel, M. B., and Mejia, A. (2021). Projection scrubbing: a more effective, data-driven fMRI denoising method. *arXiv preprint arXiv:2108.00319*.
- Power, J. D., Mitra, A., Laumann, T. O., Snyder, A. Z., Schlaggar, B. L., and Petersen, S. E. (2014). Methods to detect, characterize, and remove motion artifact in resting state fmri. *Neuroimage*, 84:320–341.
- Raymaekers, J. and Rousseeuw, P. J. (2021). Transforming variables to central normality. *Machine Learning*, pages 1–23.
- Rigby, R. A., Stasinopoulos, M. D., Heller, G. Z., and De Bastiani, F. (2019). *Distributions for modeling location, scale, and shape: Using GAMLSS in R*. CRC press.
- Ruppert, D. (2010). *Statistics and Data Analysis for Financial Engineering*. Springer. p. 118. Retrieved 2015-08-27.
- Tukey, J. W. (1957). On the comparative anatomy of transformations. *The Annals of Mathematical Statistics*, pages 602–632.
- Yeo, I.-K. and Johnson, R. A. (2000). A new family of power transformations to improve normality or symmetry. *Biometrika*, 87(4):954–959.